Ground-based FTIR observations of chlorine activation and ozone depletion inside the Arctic vortex during the winter of 1999/2000

J. Mellqvist,[1] B. Galle,[1] T. Blumenstock,[2] F. Hase,[2] D. Yashcov,[3] J. Notholt,[4] B. Sen,[5] J.-F. Blavier,[5] G. C. Toon,[5] and M. P. Chipperfield[6]

Received 9 July 2001; revised 28 December 2001; accepted 10 January 2002; published 30 August 2002.

[1] The time evolution and latitudinal distribution of ozone and chlorine species (HCl, $ClONO_2$, and ClO) in the Arctic and midlatitude stratosphere have been studied for the winter of 1999/2000. This has been done by the use of ground-based solar absorption Fourier Transform Infrared (FTIR) measurements from four locations: Harestua (60.2°N, 10.8°E), Kiruna (67.8°N, 20.4°E), Esrange (67.9°N, 21.1°E), and Ny Ålesund (79°N, 12°E). The measurements were normalized with the inert tracer HF to minimize the effects of transport, combined using the concept of equivalent latitude and interpreted using the 3D model SLIMCAT. By late January, there was strong chlorine activation with 33% of the available inorganic chlorine column (HCl + $ClONO_2$) being lost, with amounts of ClO greatly enhanced. By the middle of March, the ClO had been deactivated to $ClONO_2$, which exceeded its original fractional abundance (41%), but HCl stayed low (39%) and the ClO columns were still enhanced. The strong and sustained chlorine activations caused considerable accumulated ozone column loss of (12 ± 7)% and (31 ± 4)% by the beginning of February and March, respectively. The model showed only (5 ± 3)% and (23 ± 5)% column loss for the same time periods. By comparison, the 1998/1999 winter measurements showed no significant loss of column ozone but a 10% loss in the model. *INDEX TERMS:* 0340 Atmospheric Composition and Structure: Middle atmosphere—composition and chemistry; 3334 Meteorology and Atmospheric Dynamics: Middle atmosphere dynamics (0341, 0342); 0341 Atmospheric Composition and Structure: Middle atmosphere—constituent transport and chemistry (3334); *KEYWORDS:* Arctic, ground-based FTIR, accumulated ozone loss, chlorine activation

1. Introduction

[2] Ground-based Fourier Transform Infrared (FTIR) measurements have been conducted within the framework of the Network for Detection of Stratospheric Change (NDSC) during the last 6 years from 3 high-latitude stations situated at Harestua (60.2N, 10.8E), Kiruna (67.8N, 20.4E) and Ny Ålesund (79N, 12E). In addition, during the winter of 1999/2000 measurements were also made at Esrange (67.9N, 21.1E), near Kiruna, by the JPL MkIV interferometer [*Toon et al.*, 1992], an NDSC instrument usually operated in California, USA. This paper combines measurements from these 4 sites with results from the SLIMCAT 3D chemical transport model [*Chipperfield*, 1999]. This study will focus on chlorine partitioning and ozone depletion inside the 1999/2000 Arctic winter vortex, with some comparisons to the previous winter. By measuring the absorption lines from pressure-broadened rovibrational transitions in the infrared part of the solar spectrum, total columns of up to 25 atmospheric species can be measured by the FTIR technique. Long-lived tracers such as HF, COF_2, N_2O, and CH_4 can be measured, containing in themselves information about the total amount of diabatic descent in the polar vortex and tropopause height changes [*Galle et al.*, 1999a; *Notholt et al.*, 1997b; *Toon et al.*, 1999]. In addition, by normalizing the measured total columns of various stratospheric species (HCl, $ClONO_2$, O_3 and HNO_3) with that of HF, most of the dynamical effects by diabatic descent and tropopause height changes can be removed. This has been demonstrated in the past [*Wegner et al.*, 1998; *Toon et al.*, 1999; *Bell et al.*, 1995] but in general little quantitative information has been derived, especially for the nonchlorine species.

[3] Using data from just one site, it is difficult to separate temporal variations in the stratospheric composition from changes due to movement of the vortex. This sampling problem is compounded by the absence of winter sunlight in the far north (Ny Ålesund) and by the scarcity of prewinter vortex excursions to the far south (Harestua). In order to couple together the results at the various sites, the concept of Equivalent Latitude (EQL) has been applied, together with a 3D chemical transport model SLIMCAT. For a

[1]Radio and Space Science, Chalmers University of Technology, Göteborg, Sweden.
[2]IMK, Forschungszentrum and University Karlsruhe, Karlsruhe, Germany.
[3]Department of Atmospheric Physics, Swedish Institute of Space Physics, Kiruna, Sweden.
[4]Alfred Wegener Institute for Polar and Marine Research, Potsdam, Germany.
[5]Jet Propulsion Laboratory, California Institute of Technology, Pasadena, California, USA.
[6]School of the Environment, University of Leeds, Leeds, UK.

0148-0227/02/2001JD001080$09.00

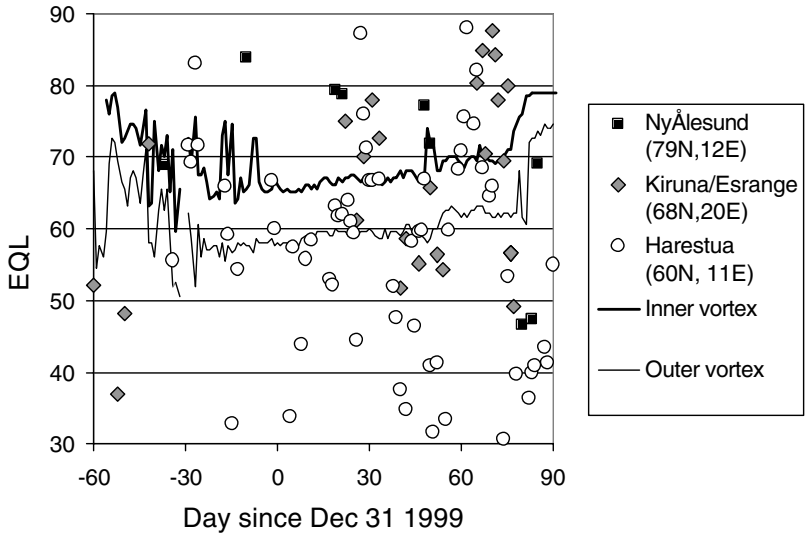

Figure 1. EQL versus time for the conducted FTIR measurements at all sites during the winter 1999/2000. Also shown are the calculated EQL of the inner and outer vortex edge.

certain potential vorticity (PV) contour, EQL is defined as the latitude of a circle which encloses the same surface area about the pole as that PV contour does around the point of most extreme PV [*Buchart and Remsberg*, 1986]. The EQL is a better tracer for air masses than just PV, since the former changes considerably less than the absolute PV over the season. If one assumes that the vortex at a given time is homogeneously distributed for air masses corresponding to the same EQL, it is then possible to quantitatively combine data from several sites probing different parts of the vortex. This is the main assumption for this paper, and as shown below, the data from the various sites yield consistent results within 5–10%. The chemical transport model results support the above approach for 1999/2000. Figure 1 shows the EQL of each site on days ground-based measurements were made during the winter 1999/2000. The EQL was calculated at University of Bremen [*Klein et al.*, 1999] from PV data obtained from the European Center for Medium Weather Forecasting (ECMWF). The inner and outer edge of the winter vortex, defined by the maxima of the second derivative of the PV versus EQL, are also plotted. The algorithm produces variable results in November and December due to the relatively weak and less confined vortex.

2. Instrument and Data Analysis

[4] The results presented here were obtained at four sites using high resolution FTIR spectrometers making ground-based solar absorption measurements [*Notholt et al.*, 1997a; *Galle et al.*, 1999a; *Blumenstock et al.*, 1997; *Toon et al.*, 1999]. Retrieved column abundances of O_3, HF, HCl, $ClONO_2$, HNO_3 and N_2O have been extensively compared to measurements made by a mobile FTIR [*Paton-Walsh et al.*, 1997; *Goldman et al.*, 1999]. Additionally, O_3 column abundances have been compared with ECC sondes, and Brewer and UV/visible spectrometers [*Mellqvist et al.*, 1999; *Lloyd et al.*, 1999] yielding agreements within 5%. At all sites spectra in different filter regions between 600 and 4500 cm^{-1}, were collected on a daily to weekly basis with variable resolutions (0.005–0.0035 cm^{-1}). During the continuous wintertime darkness the FTIR at Ny Ålesund made ground-based lunar absorption measurements with correspondingly poorer precision. Only the prewinter and late spring solar measurements from this site has been included in this study.

[5] The retrieval of total columns from the spectra can be divided into two parts, the forward model and the inverse method. The former corresponds to the physical processes (e.g., radiative transfer) relating the measured spectrum to the true atmospheric state. The atmosphere is divided into 15–70 spherical sublayers, assumed to be homogeneous. The optical depth in each layer is then calculated assuming Voigt-broadened absorption lines using spectroscopic line parameters from the HITRAN-96 database [*Rothman et al.*, 1998], ray-tracing calculations of the atmospheric path of the solar light, and pressure and temperature profiles from pT-sondes or climatological data. Since spectroscopic line parameters for $ClONO_2$ are not available, a common set of cross sections were used by all groups [*Birk and Wagner*, 2000]. Compared to the old cross sections generally used [*Ballard et al.*, 1988] the retrieved $ClONO_2$ column values were reduced by 10–35%. These new cross sections in general yield better spectroscopic fits and are more precise than the earlier ones [*Oelhaf et al.*, 2001].

[6] The inverse method is the mathematical process describing how to obtain the atmospheric state from the actual measured intensity spectrum. The standard inverse retrieval method is based on scaling an a priori volume mixing ratio (vmr) profile to minimize the residual between the spectrum calculated using the forward model, and the corresponding measured one. In addition to being scaled the stratospheric part of the vmr profile is also compressed to varying degrees and shifted in height in order to optimize the retrieval [*Toon et al.*, 1992]. It has been shown [*Paton-Walsh et al.*, 1997] that the use of a wrong concentration profile in the retrieval potentially constitutes the major

Table 1. Site Description

Site/group	Loc.	Instrument	Inv. method/code
Ny Ålesund (AWI)	79.0°N, 12.0°E	Bruker 120 HR	Standard (GGG)
Kiruna (IMK/IRF)	67.8°N, 20.4°E	Bruker 120 HR	PTM (PROFFIT)
Esrange (JPL)	67.9°N, 21.1°E	Mark IV[a]	Standard (GGG)
Harestua (CTH)	60.2°N, 10.8°E	Bruker 120 M	OEM (SFIT2) CHTW (IPR)

[a] Custom built.

source of uncertainty in the derived total columns. It is however possible to retrieve crude concentration profiles from the pressure broadened absorption spectra themselves using several inverse retrieval schemes such as the optimal estimation method (OEM) [*Rodgers*, 1976; *Connor et al.*, 1996], the Philips-Tikhnov method (PTM) [*Tikhonov*, 1963], and the Chahine Twomey method (CHTW) [*Liu et al.*, 1996; *Twomey*, 1977]; this has been done by several of the authors in this paper in order to improve the accuracy of the total columns.

[7] In Table 1 the instruments and retrieval schemes used at the different sites are given. More detailed information can be found in the papers cited in the beginning of this section. During the campaign there were two instruments measuring within 35 km of each other, at Kiruna and at Esrange. Since the instruments, data processing, retrieval software, and a priori assumptions were all different, these measurements provide a worst case estimate of the uncertainties involved. In Table 2 the mean differences between the two FTIR measurements is shown and their 1σ variability. These numbers include instrument specific systematic uncertainties and random day-to-day uncertainties, in addition to the atmospheric variability obtained since the two measurements were not entirely coincidental neither in time nor space. This variability may be considerable since the measurements were occasionally conducted during Lee wave activity, near the vortex edge, and at high solar zenith angles.

[8] The random day-to-day uncertainties correspond to systematic uncertainties that are dependent on the state of the atmosphere together with the statistical errors. The instrument specific systematic uncertainty corresponds for instance to the one associated with the tropospheric columns. Since the choice of FTIR absorption lines for ozone, HCl and HF typically have been optimized for retrieving species in the stratosphere, the measurements have little sensitivity to the lower and middle part of the troposphere, as can be shown by sensitivity modeling of the retrieval procedure [*Connor et al.*, 1996]. The tropospheric contribution obtained from the FTIR measurements is therefore influenced considerably by the a priori profile used. For the groups in this study the tropospheric contributions (column below 12 km) of HCl, HF and O_3 were 11–15%, 2–8% and 14–17% respectively, and this adds an uncertainty of several percent.

[9] In addition, Table 2 shows uncertainty estimates from several other studies together with the random day-to-day uncertainties that have been assigned to the measurements in this study. The accuracy contains the random uncertainty term together with the spectroscopic errors that assigns erroneous line strengths. This causes a multiplicative error on all the FTIR data of each species, but it neither distorts the time series nor it enhances the scatter between the stations since all the analyses used the same spectroscopic information. For the derived ratios and sums the uncertainty was obtained as the square root of the absolute uncertainties added in quadrature.

3. The 3D Model SLIMCAT

[10] The FTIR observations in this paper have been compared to SLIMCAT, an off-line 3D chemical transport model which uses meteorological analyses to specify the horizontal wind and temperature fields [*Chipperfield*, 1999]. The model uses an isentropic vertical coordinate and the diabatic descent is calculated using the MIDRAD radiation scheme [*Shine*, 1987]. In this study the model was forced using analyses from the U.K. Met. Office. The transport model is coupled to a detailed stratospheric chemistry model which integrates the usual O_x, NO_y, Cl_y, Br_y, and HO_x species along with some long-lived tracers (e.g., N_2O, CH_4). The model has 41 chemical tracers and

Table 2. Uncertainties in FTIR Column Measurements[a]

Quantity	Comparison IMK-JPL	Other studies: Random day-to-day uncertainty	Other studies: Accuracy	Random day-to-day uncertainty applied here
O_3	(6 ± 4)%	4%[b], 4%[c]	6%[b]	5%
HF	(5 ± 4)%	5.7%[d], 3%[b], 5%[c]	7.7%[d], 6%[b]	6%
HCl	(−3 ± 8)%	7.7%[d], 3%[b], 2%[c]	9.7%[d], 6%[b]	8%
$ClONO_2$[e]	(−12 ± 11)%	(9–13)%[b]	(10–14)%[b]	12%
ClO[e,f]	(−30 ± 46)%	(12–30)%[b], 23%[g]	(12–30)% [b]	20%
HNO_3	(15 ± 7)%	6.8%[d], 4%[b]	14.3%[d], 16%[b]	7%
$ClONO_2$ + HCl	(−6 ± 7)%			7%
O_3/HF	(2 ± 4)%			8%
HCl/HF	(7 ± 7)%			10%
(HCl + $ClONO_2$)/HF	(12 ± 7)%			10%

[a] A comparison between two instruments at Kiruna and Esrange, respectively, is shown in addition to other studies.
[b] Estimated from *Hase*'s [2000] study.
[c] [*Goldman et al.*, 1999].
[d] [*Paton-Walsh et al.*, 1997].
[e] The random errors for weak-absorbing species depend on the column amount and S/N.
[f] Channeling not included.
[g] [*Bell et al.*, 1996].

Table 3. Calculated Change in the HF Column Relative to a Midlatitude Reference Column of $1.2 \cdot 10^{15}$ mol · cm^{-2} Due to Compression of the Stratospheric Altitude Layers (Diabatic Descent) and Tropopause Height Changes and Corresponding Changes in Various Column Ratios (Cl = HCl + $ClONO_2$)

Modification	HF col. inc.	O_3/HF	HCl/HF	Cl/HF	HNO_3/HF	COF_2/HF
Strat. Compression						
18%	+50%	−3%	−6%	−6%	−10%	−6%
37%	+100%	−6%	−12%	−11%	−20%	−13%
58%	+150%	−9%	−17%	−17%	−29%	−20%
Δ*Tropopause height*						
−3 km	+45%	1.4%	−5.4%	−3.1%	−2.4%	−0.3%
−2 km	+30%	1.1%	−2.7%	−1.3%	−1.0%	0.1%
−1 km	+15%	0.5%	−1.4%	−0.7%	−0.5%	−0.0%
+3 km	−35%	0.5%	1.3%	0.8%	1.6%	1.7%

around 100 chemical reactions. The model also has a treatment of heterogeneous reactions on polar stratospheric clouds and sulfate aerosols. A low-resolution model run (7.5° × 7.5°) was initialized in October 1991 with output from a 2D (latitude-height) and integrated until December 1999. This simulation was then used to initialize a higher resolution (2.5 latitude × 3.75 longitude) seasonal simulation. Total stratospheric columns were output from the model for positions in the vicinity of the four measurement sites. These values have been used for both direct comparison with the measurements and as a qualitative indicator of, for example, transport processes. The model also includes a passive ozone tracer that was initialized from the modeled O_3 on 1 December and then transported without chemistry. The SLIMCAT simulation of O_3, and O_3 depletion, for this winter have been discussed by *Sinnhuber et al.* [1998]. The fluorine species HF, COF_2, and COFCl are also included in the model and since we use HF as a tracer for the dynamics in the measurements the model comparison also focused on using this species. However, to economize on computer time and memory, the model includes only two fluorine/chlorine source gases ($CFCl_3$ and CF_2Cl_2) which are scaled to obtain the correct chlorine loading. Since the average F/Cl ratio in these two species does not represent the atmospheric ratio, this in turn gives an incorrect fluorine loading and so a further scaling is applied to account for this. The model covers altitudes between about 13 to 40 km with a 1 km vertical resolution.

[11] The use of the model in this study is primarily qualitative, for interpreting the relative time evolution and geographical variation of the measurements rather than making absolute comparisons. The column values of the model have therefore been scaled, or modified with an offset, to fit midlatitude observations, occasionally without a physical justification. First, as will be shown in section 4 there are indications that the applied scaling factor for fluorine was 40% too high; this has been compensated for by dividing all fluorine species with 1.4. Second, to account for the tropospheric columns included in the FTIR data, see section 2, constant values of $4 \cdot 10^{14}$ mol · cm^{-2} and $4 \cdot 10^{17}$ mol · cm^{-2}, respectively, were added to the model HCl and ozone columns. Both numbers correspond to the average difference between the measured and modeled values over Harestua during midlatitude EQL but for HCl the number is also typical for the tropospheric contribution included in the FTIR columns. For ozone the number is 60% smaller than the anticipated tropospheric contribution. Thirdly, the midlatitude measurements of $ClONO_2$ were 25% lower than the model values. For reasons of clarity this has been compensated for in most figures, but not in Table 4, section 4.2.2, in which the chlorine partitioning of the model has been directly compared with the measurements.

4. Results and Discussion

4.1. HF as a Dynamic Tracer

[12] HF is used as a tracer in this study and this species has been discussed extensively in two previous papers [*Chipperfield et al.*, 1997; *Toon et al.*, 1999]. HF is produced by the decomposition of fluorine-containing species in the stratosphere, which also leads to the production of COF_2 and COFCl. The column of "inorganic" fluorine in the atmosphere is typically found as 50–70% HF, 20–40% COF_2 and 5–10% COFCl, depending on the latitude [*Kaye et al.*, 1991; *Mahieu and Zander*, 1999]. The two minor fluorine species are eventually photodissociated to HF, so that the COF_2/HF decreases for older air masses. When comparing air masses inside and outside the vortex this has to be accounted for since it may cause an additional decrease in the X/HF ratios inside the vortex. HF is long-lived and does not have any known sinks in the stratosphere, except outflow into the troposphere and therefore correlates well with the more often used tracer N_2O [*Toon et al.*, 1999].

4.1.1. Normalizing With HF

[13] Most of the species in this study, (HCl, $ClONO_2$, O_3 and HF) have a maximum in their number density around 18–25 km. The ground-based column measurements are therefore mostly influenced by changes at the concentration peak height, caused by, for instance dynamical effects. Since the species peak at approximately the same height and have similar concentration profile shapes up to the peak level, it is possible to remove most of dynamical effects, such as diabatic descent and tropopause height changes, by normalizing the measured total columns of various stratospheric species with HF columns. The column ratios will however still be somewhat sensitive to dynamical changes, depending on the species, since the concentration profiles are not identical in shape [*Chipperfield et al.*, 1997]. Table 3 shows the results of a simple test in which the stratospheric portion of a standard set of profiles were compressed to varying degrees in order to simulate diabatic descent [*Toon*

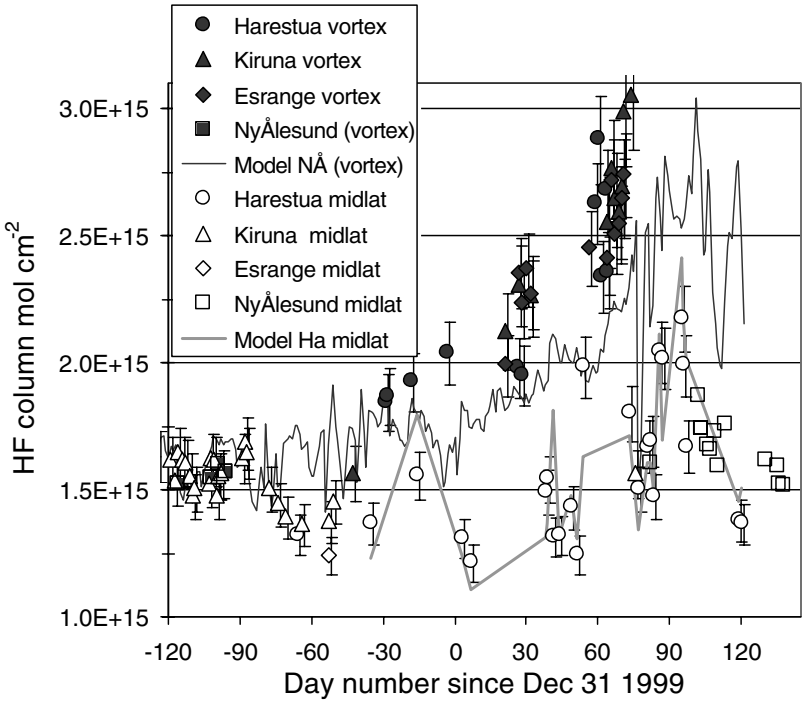

Figure 2. HF column measurements by FTIR (Harestua circles, Kiruna triangles, Esrange diamonds, and Ny Ålesund rectangles). In addition, the SLIMCAT model values (reduced by 30%) are shown for Ny Ålesund, corresponding to inside vortex and midlatitude air above Harestua.

et al., 1992] and in which the profiles were also shifted in height to simulate tropopause height changes. Standard climatological pressure and temperature profiles were used. The mean tropopause height was assumed at 10 km. Two vmr profile sets were used, a set of profiles obtained from balloon measurements [*Gaines*, 2000] and the profiles calculated by SLIMCAT for Harestua on 7 November at an EQL of 61°N. The agreement between the two profile sets was within 1–2%. It can be seen that tropopause height changes only have a small 2–3% impact on most on the ratios while diabatic descent has considerably larger effects, up to 30% for HNO_3. The same type of ratios for F_y ($\approx HF + 2 \times COF_2$) gave a slightly lower sensitivity (up to 24%) for the diabatic descent. It can be seen that the HCl/HF ratio is considerably more sensitive than the O_3/HF ratio. This is due to the fact that there is relatively more HCl in the lower stratosphere than HF and O_3 and diabatic descent will therefore change the column of HCl relatively less than for HF and O_3. However, the HCl/HF ratio is 9 times less sensitive to descent than the unratioed HCl.

[14] The SLIMCAT model can be used to assess the influence of diabatic descent since there is a passive O_3 tracer included as well as HF. We find that the modeled passive O_3/HF ratio decreased by 6% between December and March inside the vortex. During the same period the total inorganic chlorine to HF ratio declined by 10%. On the other hand, the comparison with HF showed that the diabatic descent may be slightly underestimated by the model. Nevertheless the good correlation with passive ozone shows that HF, from the model point-of-view, is a good tracer.

[15] As was mentioned above, even in the absence of chemical reactions, X/HF ratios are not strictly conserved when comparing air masses inside and outside the vortex. There is relatively more HF in the aged air at high latitudes, since a substantial fraction of the COF_2 and COFCl have then been photodissociated to HF. Measurements above Harestua has shown that the COF_2/HF ratio decreases by a factor of two in vortex air [*Galle et al.*, 1999a], from 0.22 to 0.11, and this is not believed to be caused by polar chemistry but rather photochemistry coupled with slow meridional transport. The ratios measured at Harestua are consistent with measurements at the Jungfraujoch [*Mahieu and Zander*, 1999] showing a midlatitude ratio of 0.23.

[16] The influence of the fluorine repartitioning on the X/HF column ratios can be described by equation (1). This was derived under the assumption that the fluorine reservoir, F_{sum}, corresponds to ($HF + 2COF_2$), and that the X/F_{sum} ratio is conserved, if X is chemically inert. Here the influence of COFCl has been neglected. According to equation (1) the COF_2/HF ratios measured at Harestua yields a relative decrease of about 16% in the X/HF ratios inside the vortex, compared to midlatitude air. It should be noted that the associated uncertainties with the COF_2 measurements are large due to weak absorption and limited quality assurance work conducted for this species within the NDSC.

$$\frac{(X/HF)_{vortex}}{(X/HF)_{midlat}} = \frac{1 + 2 \cdot (COF_2/HF)_{vortex}}{1 + 2 \cdot (COF_2/HF)_{midlat}} \quad (1)$$

4.1.2. HF Column Measurements

[17] In Figure 2 the measured HF columns are shown at the four sites together with the corresponding model values,

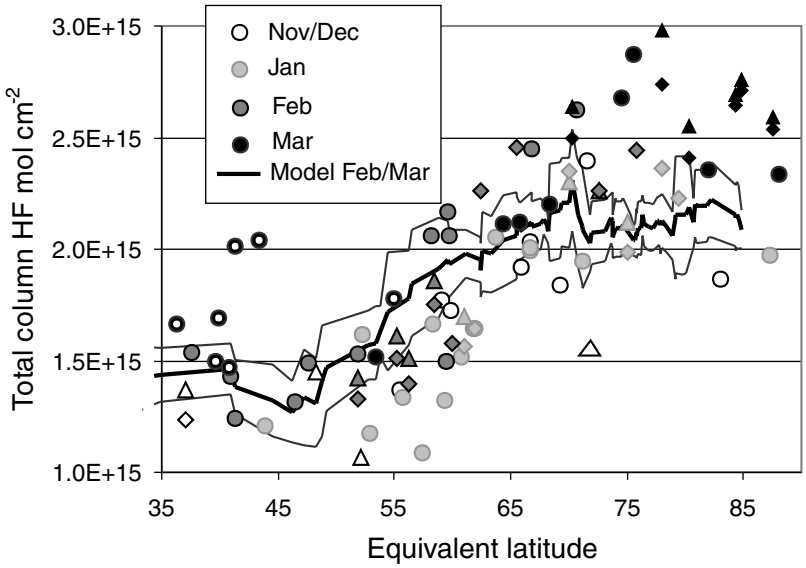

Figure 3. HF versus EQL between 19 November 1999 and 15 March 2001 measured by FTIR (Harestua circles, Kiruna triangles, and Esrange diamonds). Data after 15 March are denoted by white on black dots. In addition, the SLIMCAT model run is shown corresponding to data from all sites from 15 February to 15 March, smoothed by a running average over $\sim 1^\circ$ and their 1σ variability (lines).

divided into inner edge vortex, as defined in Figure 1 and midlatitude measurements corresponding to EQL lower than 55°. For midlatitudes the model HF values were generally 1.4 times larger than the FTIR measurements. Assuming a general error in the scaling factor for HF as was discussed in section 3, all model HF values at all sites were therefore corrected by dividing them by 1.4. These corrected HF values have been used throughout the whole paper.

[18] For Ny Ålesund the model data before day −58 correspond to the low resolution run. After reducing by 30%, the model HF values agree quite well with the midlatitude values. Inside the vortex the model seems to underestimate the increases in the HF column both in January and March. For instance the relative difference in March between the vortex and the average polar prewinter values is 60–70% for the measured and around 30–40% for the model. This may be caused by an underestimation of the diabatic descent in the model.

[19] It should be noted that SLIMCAT seems to have an inappropriate internal fluorine partitioning. The midlatitude COF_2/HF ratio is 0.11 in contrast to 0.225 as measured at the Jungfraujoch [*Mahieu and Zander*, 1999] and Harestua [*Galle et al.*, 1999a]. In the vortex the corresponding numbers are 0.07 and 0.11, for the model and measurements, respectively. The HF fraction thus seems to be overestimated in the model in general, but relatively more at midlatitudes than in polar air. Since the model HF was scaled to fit midlatitude observations, it will thus be underestimated in the polar air, and according to equation (1) the magnitude will be about 10%. However, from Figure 2 it looks as if the time evolutions of the measurements and the model, respectively, are different inside the vortex. This can not be explained by the inaccuracies in the fluorine partitioning, and is more likely due to the model underestimating the amount of diabatic descent.

[20] There is also a large discrepancy in the HF values at Ny Ålesund after day 90, some time after the final warming of the vortex, with the model up to 50% larger than the FTIR measurements. The measured air mass is of midlatitude origin since the PV values are low and since the measured O_3/HF value is around 6500, as will be discussed in section 4.3.

[21] In Figure 3 these same HF column measurements are shown versus EQL, corresponding to measurements between November 1999 and March 2000. Data after 15 March are denoted by white on black dots. In addition the SLIMCAT model HF columns are shown corresponding to 15 February to 15 March at all sites, smoothed by a running average over $\sim 1^\circ$ in EQL, together with their 1σ variability. The latter varies between 4% and 12% depending on EQL with an average variability inside the vortex corresponding to 7%. This indicates that the approach of combining different sites by using EQL is quite appropriate. As can be seen in Figure 3 the data show a distinct latitudinal dependence with a strong gradient at approximately 60° EQL. At low EQL there are a few outliers, however, these correspond to data measured after the final warming of the vortex, and may be due to vortex remnants unresolved by the model PV fields. It is also obvious from the figure that the model underestimates the HF columns in the core of the vortex.

4.2. Chlorine Activation and Partitioning

[22] The SLIMCAT model has been used here for interpreting the time evolution and latitudinal distribution of the measurements. The measured midlatitude $ClONO_2$ columns were generally 25–30% lower than the model ones. To facilitate the qualitative interpretation of the measurements the model $ClONO_2$ was reduced by 25%. This correction made the model results fit quite well to the measurements in general, over time and space. It also

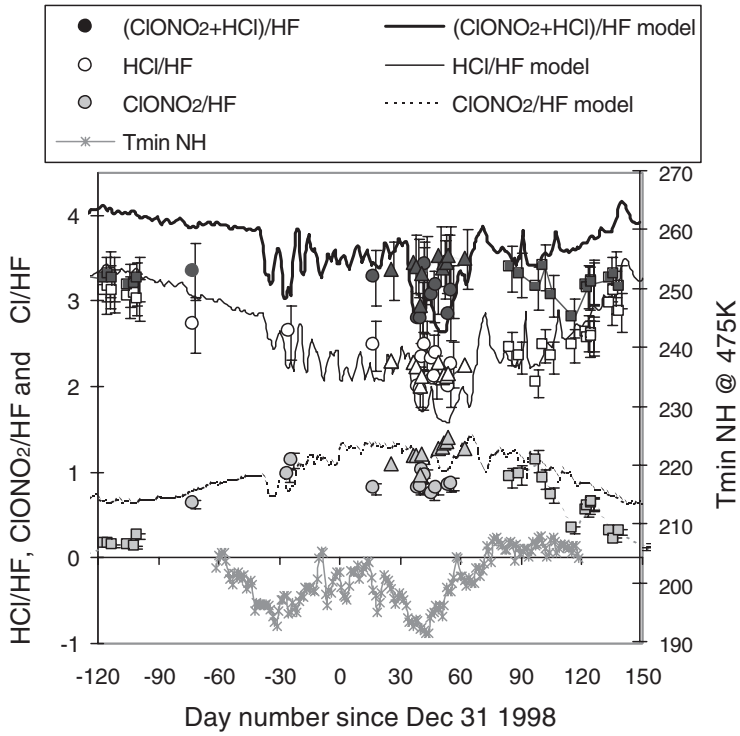

Figure 4. Time evolution of chlorine reservoir species normalized with HF at the edge and inside the polar vortex during 1998/1999, obtained by FTIR (Harestua circles, Kiruna triangles, and Ny Ålesund squares) and by the SLIMCAT low-resolution model at Ny Ålesund. The model $ClONO_2$ was reduced by 25%. Shown is also the NH minimum temperature at the 475 K surface.

improved the sum of the chlorine species ratioed to HF, as will be seen below.

4.2.1. Time Evolution and Latitudinal Distribution of the Chlorine in 1998/1999

[23] In Figure 4 the measured chlorine reservoir species normalized with HF are shown on the edge or inside the polar vortex during the earlier winter of 1998/1999, from measurements at 3 sites (Harestua, Kiruna and Ny Ålesund) and results from the low resolution SLIMCAT model corresponding to Ny Ålesund. The model values for Ny Ålesund are assumed to be characteristic for the polar vortex in general as are the inside vortex measurements at the various sites. In Figure 4 is also shown the minimum temperature at the 475 K surface in the northern hemisphere poleward of 40°N (ECMWF). For day −72 the measured O_3/HF value (4500) was used to determine that the air was of Arctic origin since PV data was not available, see section 4.3.

[24] Most of the winter/spring data correspond to measurements from Harestua and Kiruna, while the early fall and late spring data were measured from Ny Ålesund. This winter was quite warm, as can be seen in Figure 4, and in general showed little evidence of ozone depletion [*Goutail et al.*, 1999] or strong chlorine activation [*Klein et al.*, 1999]. This makes this winter ideal as a reference case when discussing the later one, 1999/2000, which showed considerably more chemical activity, in terms of ozone loss. It can also be seen that even though the FTIR measurements inside the vortex were few this winter, they corresponded to the periods when the vortex was at its coldest.

[25] Over the course of the winter the chlorine was converted from HCl into $ClONO_2$, but with the ratio of the chlorine species to HF staying almost the same (3.25 ± 0.2). Note that the variability corresponds to 6%, which is less than the estimated uncertainty level of the measurements, 10%. The HCl fraction varied between 96% to 62%. This conversion is to be expected since the production of $ClONO_2$ occurs through a termolecular reaction (ClO + NO_2 + M) while its photodissociation loss is small in the polar vortex for obvious reasons. The SLIMCAT low resolution run for Ny Ålesund, reflected the chlorine changes over time in qualitative terms, noting that the $ClONO_2$ was scaled down by 25%. During the light season (September/May) the discrepancy between the modeled and observed polar values is relatively larger, as seen in the figure.

[26] As seen from the model chlorine/HF ratios in Figure 4 there were two main periods with chlorine activation in the model in 1998/1999, around day −30 and around day 40, coinciding in time with low stratospheric temperatures. Chlorine activation was only observed significantly during one day in February, day 41, when enhanced ClO columns were measured by the FTIR over Harestua [*Galle et al.*, 1999b] as well as high OClO slant columns by a UV/visible instrument at the same site [*Van Roozendael et al.*, 1999]. In addition the chlorine/HF ratios dropped, as can be seen in the figure, but taking into account the subsidence effect, as given in Table 3, the drop was just at the threshold of the uncer-

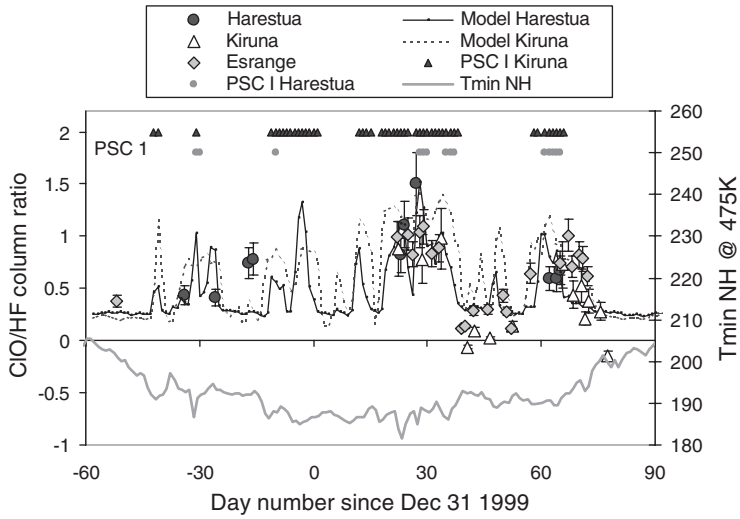

Figure 5. ClO to HF column ratios measured by FTIR, SLIMCAT model values, PSC 1 indicators, and NH minimum temperature (ECMWF) (Harestua circles, Kiruna triangles, and Esrange diamonds).

tainty level, i.e., 10%. This should be compared to the chlorine activation of the model corresponding to about 25% during the same occasions. The model used UKMO temperatures analyses which for this season seems to be 1–2 K too cold, at the lowest temperatures [*Davies et al.*, 2002]. Since the minimum temperature was just at the PSC threshold it is believed that this caused too much chlorine activation in the model.

4.2.2. Time Evolution and Latitudinal Distribution of the Chlorine in 1999/2000

[27] In Figure 5 the measured and modeled ClO/HF ratios above Kiruna, Esrange, and Harestua are shown for the winter 1999/2000. The minimum temperature at the 475 K surface in the northern hemisphere poleward of 40°N is shown (ECMWF) along with a PSC 1 flag, corresponding to days when the minimum temperatures at the 475 K surfaces were below 194.5 K above the individual sites. The minimum temperature fell below the PSC 1 threshold for the first time on day −43 and generally stayed below until day 74, when the final warming seems to have occurred.

[28] Enhanced levels of ClO are a good qualitative indicator of chlorine activation. The measurements indicate little chlorine activation around day −30 and stronger activations around the days −17, 30 and 60, respectively, which generally coincide with the periods with strong possibilities for PSC 1 formation (i.e., minimum temperatures below 194.5 K). The periods with enhanced levels of chlorine are in good qualitative agreement with the SLIMCAT model, with the exception for day −17 above Harestua. Discrepancies between the Kiruna and Esrange ClO data can be seen at several occasions, often due to the poor S/N as around day 40–45 or diurnal effects. After day 60 the Esrange instruments measured a considerably higher chlorine activation than the Kiruna instrument; this we do not fully understand. The ClO measurements have rather large uncertainties (≈23%) [*Bell et al.*, 1996], since the absorption is weak (≈1%), and for instance the Harestua instrument exhibited channeling corresponding to 1/3 of the absorption, which had to be accounted for during the spectral fitting [*Galle et al.*, 1999a]. Another problem in interpreting the ClO measurements is the exchange between ClO and Cl_2O_2, which yields a diurnal variation with maximum values of ClO around midday. Since the measurements were not always taken at midday, this adds another uncertainty to the ClO values.

[29] Figure 6 shows the measured chlorine reservoir species, normalized with HF, inside the vortex during the winter of 1999/2000 for all 4 sites together with the calculations from the SLIMCAT model for Ny Ålesund. Most of the winter/spring data correspond to measurements from the Harestua, Kiruna and Esrange sites, while the early fall and late spring data were measured from Ny Ålesund. During the fall period there were no PV fields available from ECMWF, necessary for calculating the EQL. Nevertheless, it has been assumed that the Ny Ålesund measurements are characteristic of polar stratospheric air, since they were conducted far north and were rather stable showing little variability. More importantly, the O_3/HF ratios measured at the end of September were below 5000, indicating polar air rather than midlatitude; this will be further discussed in section 4.3.

[30] At the end of September the Ny Ålesund value showed a Cl_y/HF ratio of 3.13, which was assumed to be the background reference value of the total chlorine; see further discussion below. The relative amount of HCl was then around 90%. Note that all percentage values given here have been compensated for the subsidence effect as given by the measured increase in the HF column according to Table 3. During November and December a gradual conversion of the HCl to $ClONO_2$ seem to have occurred, in the same manner as in the previous year (Figure 4). At the end of December the HCl had decreased to about 72% of the Cl_y column with the rest found as $ClONO_2$. In the end of December the model showed strong chlorine activation in contrast to the Harestua measurements. This is an artifact, however, of showing the model values for Ny Ålesund and

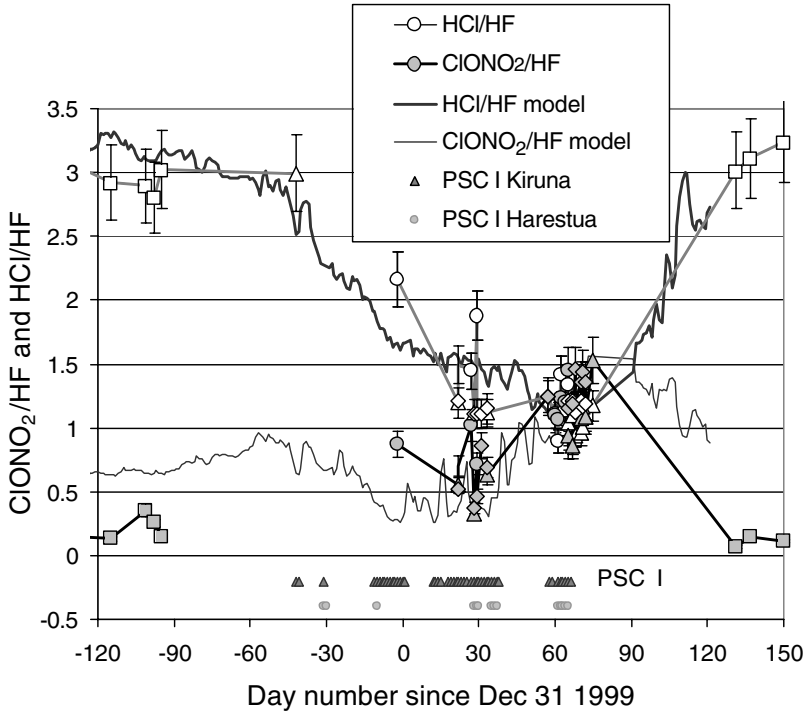

Figure 6. Time evolution of chlorine reservoir species inside the polar vortex during 1999/2000 obtained by FTIR (Harestua circles, Kiruna triangles, Esrange diamonds, and Ny Ålesund squares) and by the SLIMCAT model at Ny Ålesund. The model $ClONO_2$ was reduced by 25%. In addition, PSC 1 indicators are shown.

the measurements from Harestua; the model values for Harestua were actually in better agreement with the measurements. By the beginning of February the HCl had dropped to 44% of the Cl_y column and the $ClONO_2$ had decreased too, their sum indicating a chlorine activation of about 33% of the inorganic chlorine column. This is in reasonable agreement with the model. Compared to the measurements from the previous year the $ClONO_2$ and HCl columns were depleted by 37% and 30%, respectively. The depletion was strongest at Kiruna and Esrange, with more variability at Harestua. In early March temperatures below the PSC 1 threshold were encountered during several days above all three sites. The HCl column was still very low (39%) and similar to $ClONO_2$ (41%), which recovers much faster than HCl from the reaction of ClO with NO_2. The model recovery is in good qualitative agreement with the measurements, noting that the model $ClONO_2$ was scaled down by 25%. According to the model the low HCl in March corresponded to complete activation of this species at around 16–17 km altitude. The sum of HCl and $ClONO_2$, but also the separate ClO measurements, show that the amount of active chlorine was smaller in March than in the beginning of February, since some of the ClO had reacted with the available NO_2.

[31] In Figure 7 the various measured chlorine/HF column ratios are shown versus EQL for the winter of 1999/2000, for each month, for Harestua, Kiruna and Esrange. In addition, the corresponding SLIMCAT values are shown for all sites, together with their corresponding 1σ variability, for days between 15 February and 15 March, but smoothed by a running average over ∼1° in EQL.

[32] The measured ratios in the midlatitude air (EQL < 55°) correspond to 0.79, 2.94 and 3.74 respectively, for $ClONO_2$/HF, HCl/HF and their sum. This is consistent with midlatitude measurements at the Jungfraujoch [*Mahieu and Zander*, 1999] with ratios of 0.72, 3.08 and 3.8 during June to November. The measured average values above the Jungfraujoch in 1998 were extrapolated to year 2000 using the known trends of the halogen species.

[33] At first glance, in Figure 7, the measured column ratios of the chlorine species to HF at midlatitudes (∼3.74) are inconsistent with the background reference values measured at Ny Ålesund for the Arctic (∼3.13) and at Kiruna in September (∼3.1) in 1999 (Figure 6). Similar values (3.25 ± 0.2) were observed in 1998/1999 at several sites (Figure 4). Furthermore the same qualitative behavior has been observed by *Toon et al.* [1999], comparing measurements at Ny Ålesund (79°N) with measurements at Fairbanks (65°N) and at Lynn Lake (57°N). The reason for this discrepancy may be due to fluorine repartitioning, as mentioned in section 4.1, potentially causing a 15–20% decrease of the X/HF ratios inside the vortex. A chlorine/HF ratio of 3.74 in midlatitude air should then become 3.0–3.2 inside the vortex. Looking at the sum of $ClONO_2$ and HCl to HF in Figure 7, a gradient is indicated at 60°, where the ratio seems to drop from about 3.75 to 3.2.

[34] The model, on the other hand, does not reproduce the large variation in the chlorine/HF ratio between midlatitude and polar air. First, for Ny Ålesund in September, the sum of HCl and $ClONO_2$ to HF is much higher in the model, than in the measurements, and comparable to the midlatitude value (Figures 4 and 6). The overestimation

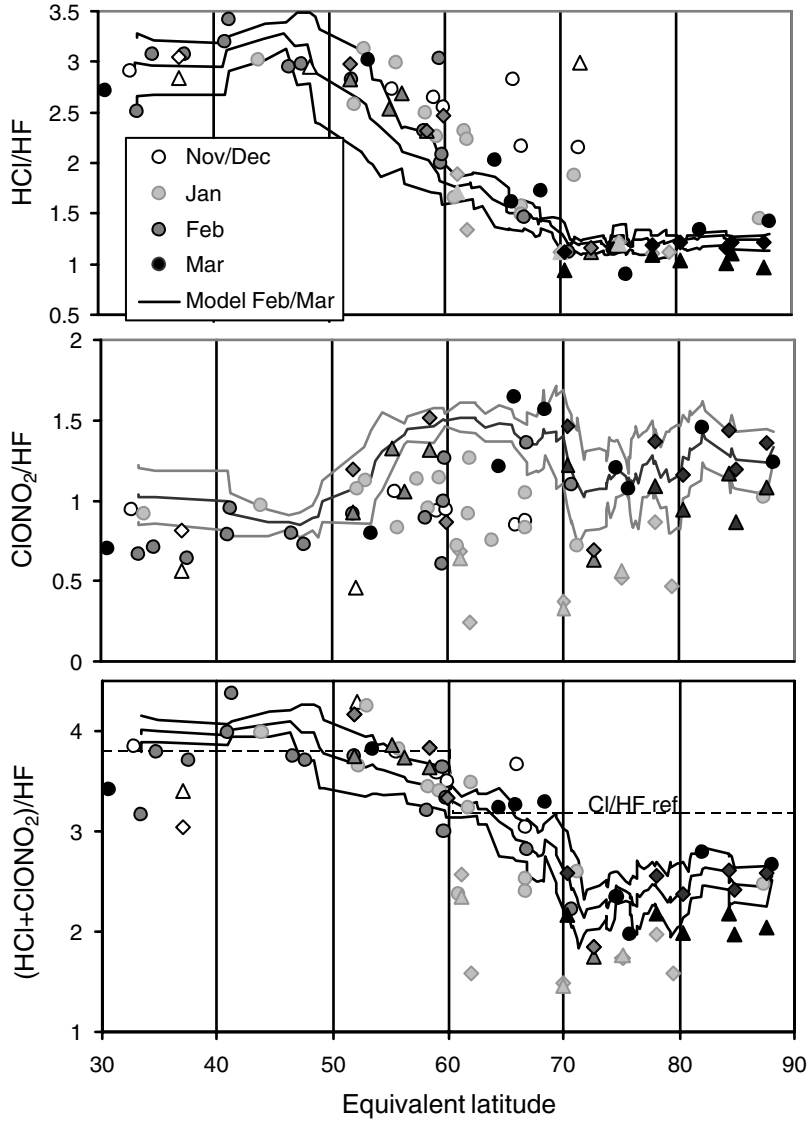

Figure 7. HCl/HF, $ClONO_2$/HF, and their sum versus EQL for 15 November to 15 March. In addition, the SLIMCAT model values for 15 February to 15 March above all sites are shown, smoothed by a running average over $\sim 1^\circ$ and their 1σ variability. The model $ClONO_2$ was reduced by 25% (Model lines, Harestua circles, Kiruna triangles, and Esrange diamonds).

corresponds to ~30% for the uncorrected values and ~23% when reducing the model $ClONO_2$ by 25%. Second, the variation in the total inorganic chlorine to HF ratio across the edge of the vortex is only 7% in the model, for December 1999. This is however anticipated, since the fluorine partitioning seems to be incorrect in the model, as discussed in section 4.1.2. Before understanding these discrepancies fully, care should be taken when using the chlorine/HF ratios from the model for quantitative interpretation.

4.2.3. Chlorine Partitioning and Comparison to the Model

[35] The relative partitioning between the measured chlorine species over the winter of 1999/2000 are directly compared with the model in Table 4. Both the measurement and model values are shown corresponding to days when the vortex was situated above Harestua, Kiruna and Ny Ålesund. The SLIMCAT values have been calculated from the chlorine species themselves and no scaling of the model values has been applied here. The measured values have been obtained by normalization with an Arctic reference value for the total chlorine to HF (~3.13), measured in September at Ny Ålesund. It is assumed that all inorganic chlorine was in HCl and $ClONO_2$ in September and this is correct within 4% according to the model. The measured X/HF ratios were compensated for subsidence by using the data in Table 3 and the corresponding HF columns. This resulted in ~6% less chlorine activation in the beginning of February and about 10% in March. In those cases when there were measurements of ClO available a corresponding Cl_2O_2 value was estimated based on the dimer-to-monomer ratio in the model multiplied with the ClO measurements. The variability of the measured values is indicated if the values correspond to several days of measurements.

Table 4. Chlorine Partitioning 1999/2000 Inside the Polar Vortex[a]

	Period	HCl%	$ClONO_2$	ClO	$2 \times Cl_2O_2$
FTS	September	92%	8%	NA	
FTS	December/January	72%	29%	NA	
FTS	January/February	(44 ± 6)%	(23 ± 8)%	(33 ± 6)%	17%
FTS	March	(39 ± 6)%	(41 ± 4)%	(22 ± 7)%	6%
Mod	September[b]	76%	20%	4%	0%
Mod	November/December	(57 ± 3)%	(22 ± 3)%	(16 ± 4)%	(5 ± 3)%
Mod	December/January	(45 ± 1)%	(21 ± 4)%	(25 ± 3)%	(9 ± 2)%
Mod	January/February	(38 ± 1)%	(18 ± 5)%	(29 ± 3)%	(15 ± 3)%
Mod	March	(31 ± 2)%	(44 ± 5)%	(19 ± 4)%	(5 ± 2)%

[a]Measured and modeled for the sites Harestua and Kiruna and Ny Ålesund. The FTIR Cl_2O_2 was estimated from the model.
[b]Low res model Ny Ålesund.

[36] As can be seen in Table 4, the model strongly overestimates the $ClONO_2$ in the Arctic in September, the partitioning almost corresponding to a midlatitude one. At the end of January and March there is good agreement between the model and the measurements. The chlorine sum for the FTIR measurements, including the estimated Cl_2O_2, indicates an unreasonably high chlorine amount (106–117%) occasionally, but this probably reflects the accuracy of the measurements, being especially poor in cases with high abundance of ClO.

[37] The vortex values in Table 4 should be compared to the average midlatitude partitioning of HCl and $ClONO_2$ over the season for the measurements [(77 ± 5)% and (21 ± 5)%] and for the model, [(65 ± 7)% and (30 ± 6)%]. Note that the model overestimates the $ClONO_2$ partitioning (by 50%) at midlatitudes as was found also for the $ClONO_2$ column in the last section.

4.3. Ozone Depletion

[38] In order to investigate the amount of ozone depletion inside the vortex we use the O_3/HF ratio, as was partly discussed in section 4.1. The O_3/HF ratio has a strong latitudinal gradient: the HF column increases by a factor of 8 between the equator and the pole while column ozone only increases by a factor of 2 [*Toon et al.*, 1999]. HF is low at the tropics due to dynamic ascent and due to a significant part of the fluorine being in the form of COF_2 and COFCl. HF does not have a stratospheric sink and so toward the poles the species increases by diabatic descent, in addition to the formation of HF from COF_2, and COFCl as discussed previously. O_3 on the other hand, shows the same type of behavior but has sinks, which significantly mitigates the "dynamical" increase. Both species have similarly shaped vertical concentration profiles in the lower stratosphere and therefore taking the O_3/HF ratio removes the effect of vertical transport to first order. As long as the vortex is strong with only small mixing of the outside air, as seems to have been the case in 1999/2000, changes in the O_3/HF ratio are a good indicator of chemical activation. The problem of calculating the accumulated O_3 loss inside the vortex then simplifies to establishing the prewinter conditions, when the vortex spins up in October/November, and then to measure the decline in the O_3/HF ratio.

[39] In Figure 8 the O_3/HF ratios measured at three sites for the winter 1998/1999 are shown together with the SLIMCAT low resolution multiannual run for Ny Ålesund

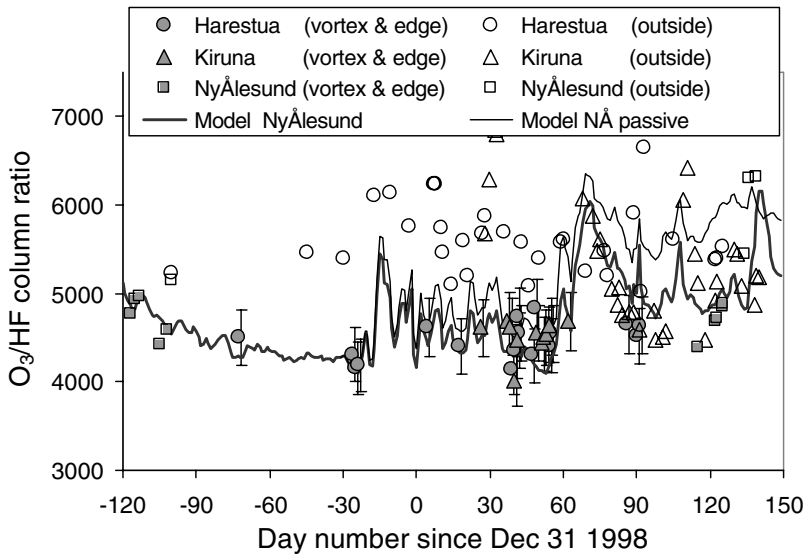

Figure 8. O_3/HF values for 1998/1999 on the edge and inside the vortex for three different sites. The low-resolution multiannual SLIMCAT model run is shown for Ny Ålesund.

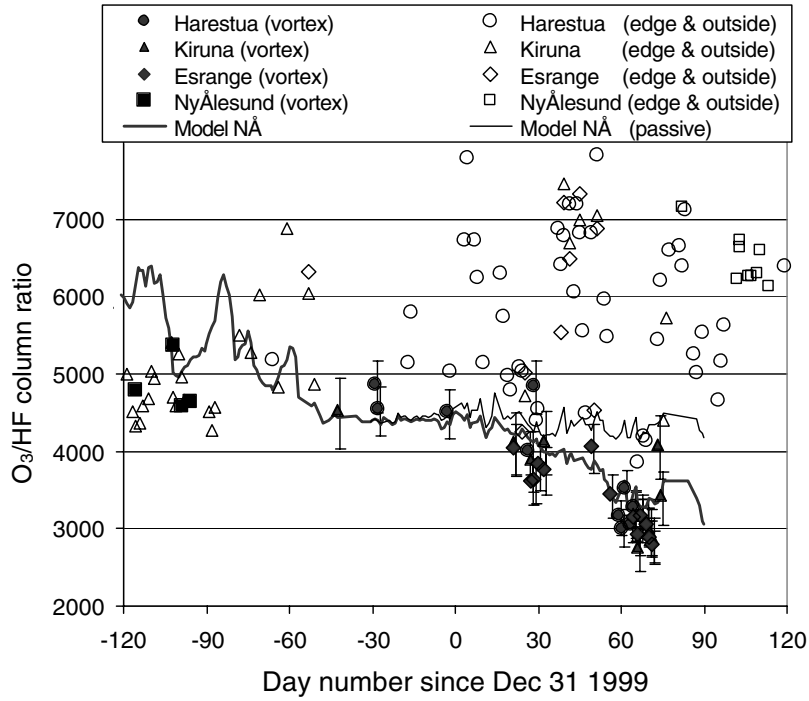

Figure 9. O_3/HF values for 1999/2000 corresponding to inside vortex (dark) and outside vortex (white), obtained by FTIR measurements and by the SLIMCAT model (passive and active O_3) at Ny Ålesund.

(active and passive ozone). An offset of $4 \cdot 10^{18}$ mol $\cdot$ cm^{-2} has been added to the model ozone to account partly for the tropospheric contribution of the FTIR columns, as was discussed in sections 2 and 3 and this applies to all figures. It can be seen that the ratios on the edge and inside the polar vortex were about the same, ~4500, at the end of September, early December and later in February/March, in general indicating no substantial accumulated O_3 loss over the course of the winter. In the measurements there are a few possible indications of O_3 loss around day 40, but at the threshold of uncertainty. This is consistent with other studies reporting that this winter generally showed little evidence of O_3 depletion [*Goutail et al.*, 1999]. The model yields similar O_3/HF values as the FTIR measurements but indicates a 10% ozone loss by the end of February. The discrepancy between measurements and model may be due to the fact that the model used UKMO temperatures, yielding too much chlorine activation as discussed in

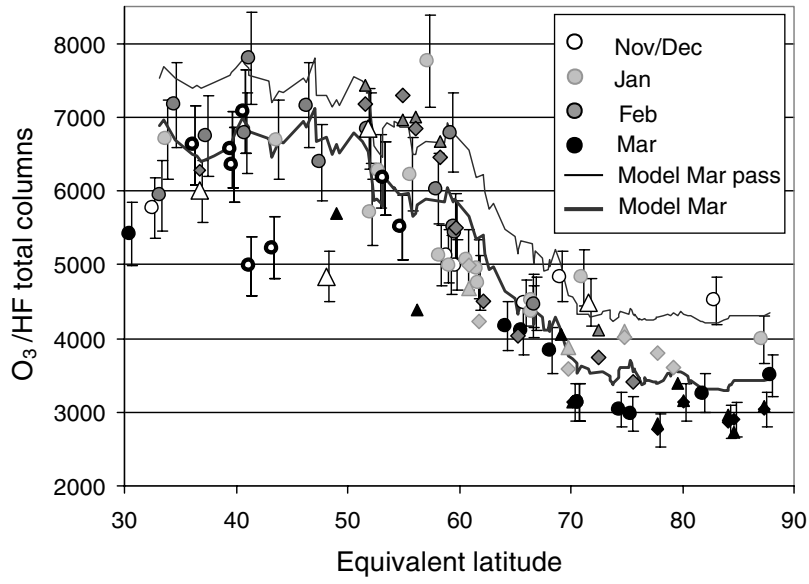

Figure 10. O_3/HF versus EQL and smoothed SLIMCAT data (running average over ~1°) corresponding to passive (gray line) and active (dark line) O_3/HF ratios above all sites during March (Model lines, Harestua circles, Kiruna triangles, and Esrange diamonds).

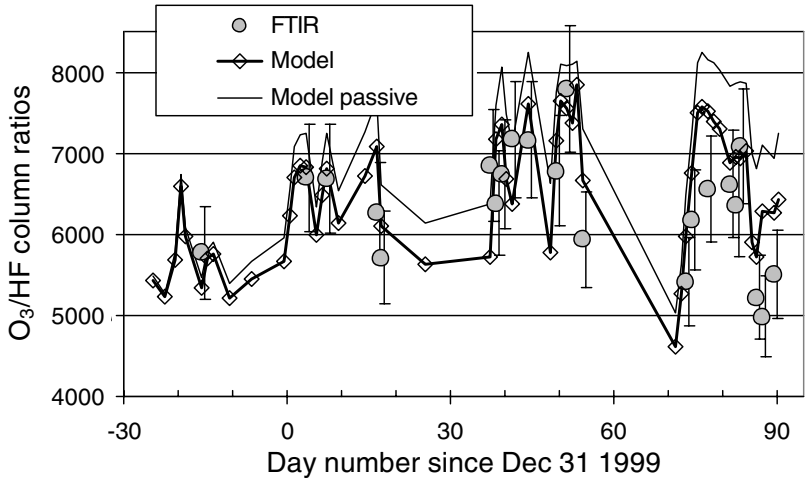

Figure 11. O_3/HF values for 1999/2000 corresponding to midlatitude air above Harestua, obtained by FTIR and from the SLIMCAT model (passive and active O_3) at Harestua.

section 4.2. From the HF columns (not shown) it can be deduced that the subsidence in general was larger in February 1998/1999 than in February 2000/2001, as can be expected due to the warmer temperatures in the earlier winter (Figure 4). This implies that the sensitivity of the O_3/HF ratios to the subsidence are within the uncertainty of the measurements. This is also in agreement with the sensitivity calculations in Table 3.

[40] In Figure 9 the O_3/HF ratios for the 1999/2000 winter are shown versus time for each site, both for the measurements and the model runs (lines). The observations have been divided into inside and edge/outside vortex, respectively, according to their EQL and the HF in the model values have been decreased by 30%, as described in section 4.1. In addition, the passive O_3/HF ratios are shown for Ny Ålesund. It can be seen that the Ny Ålesund values converged toward 4500 in late September, in good agreement with both the Kiruna and Harestua data measured later in November and December. This indicates that there was probably no significant mixing of midlatitude air into the vortex in October/November, since the ratio would then have increased. The model values on the other hand indicate a slight decrease (10%) in the ratios between September and the middle of November. According to PV data the high O_3/HF values at Ny Ålesund in the end of April corresponded to inflow of midlatitude air, occurring after the final warming of the vortex, around day 74.

[41] In Figure 10 the measured O_3/HF ratio at all sites are shown versus EQL. In addition, the SLIMCAT ratios are shown for the Harestua site for all days in March, both for the active and passive O_3. The model values were smoothed by a running average over $\sim 1^\circ$ in EQL and had a 1σ variability of about 13% outside the vortex and 3% inside. The strong dependence of the O_3/HF ratio with EQL is apparent. It can be seen that an O_3/HF ratio of 5000 is a good threshold for distinguishing vortex edge air directly from the measurements itself, since the EQL is then 60^o or larger. Correspondingly an O_3/HF ratio of 5500 or higher seems to indicate the presence of midlatitude air. By the beginning of March low column ratios of approx. 3000 were quite homogeneously distributed within the vortex, independent of EQL and measurement site. By the end of March, around day 90, after the final warming around day 74, there were O_3/HF ratios outside the vortex (white on black dots) that were considerably lower than those predicted by the model. The model in general showed ozone loss also at midlatitudes in the end of March (13%), as can be seen from the difference in the O_{3pass}/HF and O_3/HF ratios in Figure 10. This is even more clear in Figure 11, which shows the midlatitude measurements and model values above Harestua. The measurements actually showed even more loss than the model (25%), calculated from the average ratios at the same EQL values. These low ozone values probably correspond to polar air masses, which have mixed with midlatitude air, since they appear only after the break up of the vortex. These values also correspond to the outlier points apparent in Figure 3 with high HF column values at midlatitudes.

[42] Figure 12 shows the deduced ozone depletion obtained from the seasonal decline in the measured O_3/HF values above Harestua and Kiruna, together with the corresponding data calculated by the SLIMCAT model. In addition, the model values for O_3 normalized with the passive O_3 tracer are shown for Ny Ålesund, corresponding directly to the ozone depletion. The error bars shown correspond to the precision of single measurements; the ensemble averages should be more precise. The measured ratios have been compensated for the effect of subsidence according to section 4.1, which reduced the apparent O_3 depletion by 2–4%. Noteworthy conclusions are: The measurements showed an accumulated ozone loss of (12 ± 7) by the end of January and (31 ± 4)% by the beginning of March, which corresponds to ozone column losses of 42 ± 24 DU and 135 ± 33 DU, respectively. This should be compared to the values obtained by the model of (5 ± 3)% and (23 ± 5)%. Thus the model shows lower column ozone depletion in both January and March with the largest relative difference in January. The model calculation also showed that it was appropriate to use the decline in the O_3/HF values above each station to calculate the ozone loss, since the decline in the O_3/O_3(passive) ratios above Ny Ålesund gave very similar results, within a few percent.

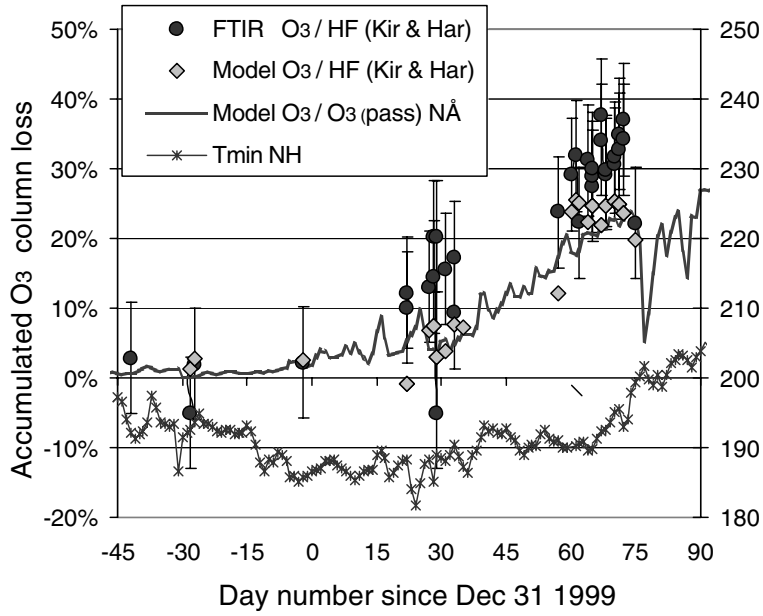

Figure 12. Accumulated ozone column loss inside the polar vortex deduced from the decline in the measured O_3/HF ratio at Kiruna and Harestua (black). The corresponding results are shown for SLIMCAT (gray). In addition, the decline in the O_3/O_3 (passive) ratio at Ny Ålesund is shown (thick line) as well as the minimum temperature at the 475 K surface in the Northern Hemisphere obtained from ECMWF.

[43] In a recent comparison of empirical ozone loss studies during the 1999/2000 winter [*Harris et al.*, 2002], column ozone losses varying between 80–105 DU were shown in March. This is 20–40% lower ozone column loss than we found in this study and in January there are no reports of ozone depletion by these studies.

[44] Noteworthy is that the magnitude of the column losses in the other studies are similar to the accumulated ozone column loss between January and March (93 DU) in this study. Most of the other studies relied on transport calculations driven by meteorological analyses, in contrast to this study relying on an O_3-tracer relationship.

[45] Possible reasons for an overestimation of the column ozone loss in this study is either, that the subsidence causes larger decreases in the X/HF ratios than estimated in Table 3 or, that the O_3/HF reference value used for the polar vortex was too high. The first reason is not likely since the measurements in 1998/1999, during which the subsidence was larger than in 1999/2000, indicate that the subsidence effect is within 10% for O_3/HF, which is consistent with Table 3. Regarding the O_3/HF reference values measured at Ny Ålesund in September, the SLIMCAT model actually indicates a 10% decrease of the O_3/HF ratio until the end of November (Figure 9). Such a decrease is not seen in the measured data, however, but on the other hand the number of measurements in November and December were few. Considering the measurement precision, part of the discussed discrepancy (17–34 DU) could be explained, assuming the decrease in the SLIMCAT model to be correct.

5. Summary and Conclusion

[46] In this paper measurements made by intercalibrated FTIR instruments located at different sites have been combined using the concept of equivalent latitude. A 3D chemical transport model (SLIMCAT) has been used in parallel with the measurements, to facilitate interpretation of the results and to better understand the limitations of this approach. The results show that combining results from various sites, measuring both inside and outside the polar vortex, provides a more comprehensive view of the chemical evolution of the vortex. It also enables a better distinction between the temporal and latitudinal properties of the vortex, which are difficult to separate when using data from a single site. The plots of X/HF ratios versus EQL showed distinct relationships, independent of measurement site, reflecting the dominant meridional dependence of the various species, with the strongest gradients obtained at the vortex edge around 60°N. It was also shown that the magnitude of the O_3/HF ratio may be used as tracer for vortex air and midlatitude air, corresponding to threshold values of 5000 and 5500, respectively.

[47] The SLIMCAT model in general reproduced the latitudinal characteristics of the measured species to HF ratios, in qualitative terms. The model showed too large $ClONO_2$ columns (30–40%), both in the Arctic and at midlatitudes, with relatively more overestimation during the sunlit season in September and May. This could also be seen in the chlorine partitioning. In addition, the measured sum of the chlorine reservoirs normalized with HF showed a 16% decrease between the outside and inside of the polar vortex, but the model only reproduced a 7% decrease. The model also showed 40% too high HF values, at midlatitudes but the relative increase of HF due to subsidence during the evolution of the vortex was underestimated by 20–30%. This indicates a possible underestimation of the subsidence, which also should affect the passive ozone, sometimes used as a baseline when calculat-

ing ozone loss from absolute ozone measurements. On the other hand, part of this effect could be mitigated by the fact that the fluorine partitioning in the model was incorrect showing an overestimation of the relative abundance of HF.

[48] During the winter of 1998/1999 the temperature was generally above the PSC 1 threshold, with some exceptions. Most measurements on the edge and inside the vortex showed only the anticipated gas-phase repartitioning of the HCl to $ClONO_2$ over the course of the winter, with the HCl fraction varying between 95% to 67%. The chlorine/HF ratio corresponded to 3.25 ± 0.2 inside the vortex. The O_3/HF ratios generally stabilized around 4500. There was one day with observations of significant chlorine activation, coinciding with enhanced ClO and a drop in the O_3/HF ratios. However, in general most measurements showed evidence of small activation, within the 8–10% uncertainty level of the measurements. This is in contrast to the SLIMCAT model showing in general larger chlorine activation and ozone loss.

[49] During 1999/2000 the minimum temperature in the vortex was persistently below the PSC threshold temperature (194.5 K) from December until the end of March. During this period the HCl was first converted to $ClONO_2$, through standard gas phase chemistry, as occurred also in 1998/1999. Then in February and March strong chlorine activation was observed, consistent with more or less complete depletion at the peak height for HCl, according to the model simulations. The chlorine activation was both observed by direct ClO measurements and also by observations of the decline of the normalized reservoir species (HCl, $ClONO_2$). These measurements are thus consistent with that considerable PSC processing was going on in the vortex in February and March. In January the chlorine reservoir species corresponded to 67% of the chlorine column with the rest being active chlorine. This coincided with ozone depletion of 12%, which was twice what the model calculated. In March the column $ClONO_2$ increased, opposite to the active chlorine which decreased, most likely through the reaction of ClO with NO_2. The HCl remained slightly lower than in February (39%). The accumulated ozone loss was now 31%, which was higher than the model simulation showing 23% depletion.

[50] **Acknowledgments.** We thank Ulf Klein University of Bremen for providing us with the EQL calculations, Brian Connor (NIWA) and Curtis Rinsland (NASA Langely) for SFIT2, University of Denver for IPR and DNMI, and NILU for pT-sonde data. DG-XII of the European Community is acknowledged for funding the THESEO 2000 campaign under the contracts ENV4-CT-1998-0750, EVK2-CT-1999-00047, and EVK2-CT-1999-000049. We also acknowledge Goddard Space Flight Center for pressure and temperature profiles of the National Center for Environmental Prediction via the automailer system. We thank our engineers C. Wille and N. Spelten for performing the FTIR-observations in Ny Ålesund. The modeling work was supported by the U.K. Natural Environment Research Council. Some of the data used in this publication were obtained as part of the Network for the Detection of Stratospheric Change (NDSC) and are publicly available (see http://www.ndsc.ws).

References

Ballard, J., W. B. Johnston, and M. R. Gunson, Absolute absorption coefficients of ClONO2 infrared bands at stratospheric temperature, *J. Geophys. Res.*, *93*, 1659–1665, 1988.

Bell, W., et al., FTIR measurements of HCl, $ClONO_2$, ClO, HF, HNO_3 over Aberdeen and comparison with a 3D model, in *Proceedings of the Third European Workshop on Polar Stratospheric Ozone*, Schliersee, edited by J. A. Pyle et al., pp. 399–402, Eur. Comm., Luxembourg, 1995.

Bell, W., C. Paton-Walsh, T. D. Gardiner, P. T. Woods, N. R. Swann, N. A. Martin, L. Donohoe, and M. P. Chipperfield, Measurements of stratospheric chlorine monoxide (ClO) from groundbased FTIR observations, *J. Atmos. Chem.*, *24*, 285–297, 1996.

Birk, M. and G. Wagner, A new spectroscopic database for chlorine nitrate, paper presented at the 6th HITRAN Conference, Cambridge, USA, 2000.

Blumenstock, T., H. Fischer, A. Friedle, A. F. Hase, and P. Thomas, Column amounts of $ClONO_2$, HCl, HNO_3, and HF from ground-based FTIR measurements made near Kiruna, Sweden, in late winter 1994, *J. Atmos. Chem.*, *26*, 311–321, 1997.

Buchart, N., and E. E. Remsberg, The area of the stratospheric polar vortex as a diagnostic for tracer transport on an isentropic surface, *J. Atmos. Sci.*, *43*, 1319–1339, 1986.

Chipperfield, M. P., Multiannual simulations with a three-dimensional chemical transport model, *J. Geophys. Res.*, *104*, 1805–1881, 1999.

Chipperfield, M. P., et al., On the use of HF as a reference for the comparison of stratospheric observations and models, *J. Geophys. Res.*, *102*, 12,901–12,919, 1997.

Connor, B. J., N. B. Jones, S. W. Wood, J. G. Keys, C. P. Rinsland, and F. J. Murcray, Retrieval of HCl and HNO_3 profiles from ground-based FTIR data using SFIT2, in *Proceedings of the XVIII Quadrennial Ozone Symposium*, pp. 485–488, l'Aquila, edited by R. D. Bojkov and G. Visconti, Int. Ozone Comm., World Meteorol. Org., Geneva, Switzerland, 1996.

Davies, S., et al., Modeling the effect of denitrification on Arctic ozone depletion during winter 1999/2000, *J. Geophys. Res.*, *107*, 10.1029/2001JD000445, in press, 2002.

Gaines, S., SOLVE mission dataset [CD-ROM, NASA/UARP-0009], NASA Ames Res. Cent., Moffett Field, Calif., 2000.

Galle, B., J. Mellqvist, D. W. Arlander, I. Flöisand, M. P. Chipperfield, and A. Lee, Ground based FTIR measurements of stratospheric trace species from Harestua, Norway during sesame and comparison with a 3-D model, *J. Atmos. Chem.*, *32*, 147–164, 1999a.

Galle, B., J. Mellqvist, J. Samuelsson, S. Magnusson, M. Van Rosendael, C. Fayt, F. Hendrick, M. P. Chipperfield, and A. Bjerke, FTIR and UV-visible measurements of stratospheric trace species at Harestua, Norway during THESEO and comparison with a 3-D model, in *Proceedings of Stratospheric Ozone 1999*, pp. 240–243, Saint Jean de Luz, edited by N. R. P. Harris et al., Eur. Comm., Luxembourg, 1999b.

Goldman, A., C. Paton-Walsh, W. Bell, G. C. Toon, J.-F. Blavier, B. Sen, M. T. Coffey, J. W. Hannigan, and W. G. Mankin, Network for the detection of stratospheric change Fourier transform infrared intercomparison at Table Mountain Facility, November 1996, *J. Geophys. Res.*, *104*, 30,481–30,503, 1999.

Goutail, F., J. P. Pommerau, and F. Lefevre, Winter ozone loss in the Arctic and at mid-latitude in 1998 and 1999 from the SAOZ ground-based network and balloon measurements, in *Proceedings of Stratospheric Ozone 1999*, pp. 433–437, Saint Jean de Luz, edited by N. R. P. Harris et al., Eur. Comm., Luxembourg, 1999.

Hase, F., Inversion von Spurengas-profilen aus hochaufgelösten bodengebunden FTIR-Messungen in Absorption, ISSN 0947-8620, *Tech. Rep. FZKA 6512*, 148 pp., Forsch. Karlsruhe, Karlsruhe, 2000.

Harris, N. R. P., M. Rex, F. Goutail, B. M. Knudsen, G. L. Manney, R. Muller, and P. von der Gathen, Comparison of empirically derived ozone losses in the Arctic vortex, *J. Geophys. Res.*, *107*, 10.1029/2001JD000482, in press, 2002.

Kaye, J. A., A. R. Douglass, C. H. Jackman, R. S. Stolarski, R. Zander, and G. Roland, Two dimensional model calculations of fluorine containing reservoir species in the stratosphere, *J. Geophys. Res.*, *96*, 12,865–12,881, 1991.

Klein, U., B. Barry, K. Lindner, I. Wohltmann, and K. F. Kunzi, Observations of polar stratospheric chlorine monoxide in Ny-Ålesund, Spitsbergen, 1998 and 1999, in *Proceedings of Stratospheric Ozone 1999*, pp. 272–275, Saint Jean de Luz, edited by N. R. P. Harris et al., Eur. Comm., Luxembourg, 1999.

Liu, X., F. J. Murcray, and D. G. Murcray, Comparison of HF and HCl vertical profiles from ground-based high resolution infrared solar spectra with Halogen Occultation Experiment observations, *J. Geophys. Res.*, *101*, 10,175–10,181, 1996.

Lloyd, S., et al., Intercomparison of total ozone observations at Fairbanks, Alaska, during POLARIS, *J. Geophys. Res.*, *104*, 26,767–26,778, 1999.

Mahieu, E. and R. Zander, Fifteen years-trend characteristics of key stratospheric constituents monitored by FTIR above the Jungfraujoch, in *Proceedings of Stratospheric Ozone 1999*, pp. 99–182, Saint Jean de Luz, edited by N. R. P. Harris et al., Eur. Comm., 1999.

Mellqvist, J., B. Galle, J. Samuelsson, and S. Magnusson, Height resolved ground based FTIR measurements above Harestua, Norway during 1995 to 1999, in *Proceedings of Stratospheric Ozone 1999*, pp. 284–286, Saint Jean de Luz, edited by N. R. P. Harris et al., Eur. Comm., Luxembourg, 1999.

Notholt, J., G. C. Toon, R. Lehmann, B. Sen, and J.-F. Blavier, Comparison

of Arctic and Antarctic trace gas column abundances from ground-based Fourier transform infrared spectrometry, *J. Geophys. Res.*, *102*, 12,863–12,869, 1997a.

Notholt, J., G. C. Toon, F. Stordal, S. Solberg, N. Schmidbauer, E. Becker, A. Meier, and B. Sen, Seasonal variations of atmospheric trace gases in the high Arctic at 79 degrees N, *J. Geophys. Res.*, *102*, 12,855–12,861, 1997b.

Oelhaf, H., et al., Interconsistency checks of ClONO2 retrievals from MIPAS-B spectra by using different bands and spectroscopic parameter sources, in *Proceedings of IRS 2000: Current Problems in Atmospheric Radiation*, pp. 615–618, edited by W. L. Smith and Yu. M. Timofeyev, A. Deepak, Hampton, Va., 2001.

Paton-Walsh, C., W. Bell, T. Gardiner, N. Swann, P. Woods, J. Notholt, H. Schutt, B. Galle, W. Arlander, and J. Mellqvist, An uncertainty budget for ground-based Fourier transform infrared column measurements of HCl, HF, N_2O, and HNO_3, deduced from results of side-by-side instrument intercomparisons, *J. Geophys. Res.*, *102*, 867–887, 1997.

Rodgers, C. D., Retrieval of atmospheric temperature and composition from remote measurements of thermal radiation, *Rev. Geophys. Space Phys.*, *14*, 609–624, 1976.

Rothman, L. S., et al., The HITRAN molecular database and HAWKS (HITRAN atmospheric workstation) 1996 edition, *J. Quant. Spectrosc. Radiat. Transfer*, *60*, 665–710, 1998.

Shine, K. P., The middle atmosphere in the absence of dynamical heat fluxes, *Q. J. R. Meteorol. Soc.*, *113*, 603–633, 1987.

Sinnhuber, B.-M., et al., Large Loss of total ozone during the Arctic winter of 1999/2000, *Geophys. Res. Lett.*, *27*, 3473–3476, 2000.

Tikhonov, A. N., On the solution of incorrectly stated problems and a method for regularization, *Acad. Nauk., USSR*, *151*, 501–504, 1963.

Toon, G. C., et al., Evidence for subsidence in the 1989 Arctic winter stratosphere from airborne infrared composition measurements, *J. Geophys. Res.*, *97*, 7963–7970, 1992.

Toon, G. C., J.-F. Blavier, B. Sen, R. J. Salawitch, G. B. Osterman, J. Notholt, M. Rex, C. T. McElroy, and J. M. Russel III, Ground-based observations of Arctic O_3 loss during spring and summer 1997, *J. Geophys. Res.*, *104*, 26,497–26,510, 1999.

Twomey, S. S., Some aspects of the inversion problem in remote sensing, in *Proceedings of Inversion Methods in Atmospheric remote sounding*, pp. 41–65, A. Deepak, Hampton, Va., 1977.

Van Roozendael, M., C. Fayt, F. Hendrick, C. Hermans, J.-C. Lambert, D. Fonteyn, B.-M. Sinnhuber, and M. Chipperfield, Seasonal and diurnal variations of BrO column abundances above Harestua (60N) and Haute-Provence (44N) during THESEO, in *Proceedings of Stratospheric Ozone 1999*, pp. 332–335, Saint Jean de Luz, edited by N. R. P. Harris et al., Eur. Comm., Luxembourg, 1999.

Wegner, A., G. P. Stiller, T. von Clarmann, G. Maucher, T. Blumenstock, and P. Thomas, Sequestration of HNO_3 in polar stratospheric clouds and chlorine activation as monitored by ground-based Fourier transform infrared solar absorption measurements, *J. Geophys. Res.*, *103*, 22,181–22,200, 1998.

B. Galle and J. Mellqvist, Radio and Space Science, Chalmers University of Technology, S-41296 Göteborg, Sweden. (johan.mellqvist@rss.chalmers.se)

T. Blumenstock and F. Hase, IMK, Forschungszentrum and University Karlsruhe, Karlsruhe, Germany.

D. Yashcov, Swedish Institute of Space Physics, Kiruna, Sweden.

J. Notholt, Alfred Wegener Institute for Polar and Marine Research, Potsdam, Germany.

J.-F. Blavier, B. Sen, and G. C. Toon, Jet Propulsion Laboratory, California Institute of Technology, Pasadena, CA, USA.

M. P. Chipperfield, School of the Environment, University of Leeds, Leeds, UK.